

Exploration of LICA Detections in Resting State fMRI

Darya Chyzhyk¹, Ann K. Shinn², and Manuel Graña¹

¹ Computational Intelligence Group
Dept. CCIA, UPV/EHU, Apdo. 649, 20080 San Sebastian, Spain
www.ehu.es/ccwintco

² McLean Hospital, Belmont, Massachusetts; Harvard Medical School,
Boston, Massachusetts, US

Abstract. Lattice Independent Component Analysis (LICA) approach consists of a detection of lattice independent vectors (endmembers) that are used as a basis for a linear decomposition of the data (unmixing). In this paper we explore the network detections obtained with LICA in resting state fMRI data from healthy controls and schizophrenic patients. We compare with the findings of a standard Independent Component Analysis (ICA) algorithm. We do not find agreement between LICA and ICA. When comparing findings on a control versus a schizophrenic patient, the results from LICA show greater negative correlations than ICA, pointing to a greater potential for discrimination and construction of specific classifiers.

1 Introduction

Many works on fMRI analysis are based on the Independent Component Analysis (ICA) [18]. The approaches to solve the ICA problem obtain both the independent sources and the linear unmixing matrix. These approaches are unsupervised because no *a priori* information about the sources or the mixing process is included, hence the alternative name of Blind Deconvolution. Spatial sources in fMRI correspond to the activations localizations in the brain volume, while temporal sources correspond to statistical independent patterns of BOLD signal intensities. The main advantage of ICA is that it does not impose a priori assumptions on the selection of observations, thus avoiding “double dipping” effects biasing the results. We have used the FastICA algorithm implementation available at [1].

We have proposed Lattice Independent Component Analysis (LICA) [7] a Lattice Computing [6] approach that we call that consists of two steps. First it selects Strong Lattice Independent (SLI) vectors from the input dataset using an incremental algorithm, the Incremental Endmember Induction Algorithm (IEIA) [11]. Second, because of the conjectured equivalence between SLI and Affine Independence [9], it performs the linear unmixing of the input dataset based on these endmembers. We assume that the data is generated as a convex combination of a set of endmembers which are the vertices of a convex polytope

covering some region of the input data. This assumption is similar to the linear mixture assumed by the ICA approach, however we do not impose any probabilistic assumption on the data. Endmembers correspond to the ICA's temporal independent sources. LICA is unsupervised, as ICA, and it does not impose any a priori assumption on the data. We have applied LICA to fMRI activation detection [8,7], and Voxel Based Morphometry of structural MRI [2]. In this paper we explore its application to resting state fMRI.

The outline of the paper is as follows: Section 2 reviews resting state fMRI. Section 3 overviews the LICA. Section 4 presents results of LICA versus ICA on small case study. Section 5 provides some conclusions.

2 Resting State fMRI Background

Resting state fMRI data has been used to study the connectivity of brain activations [4,13,17]. The assumption is that temporal correlation of low frequency oscillations in diverse areas of the brain reveal their functional relations. When no explicit cognitive task is being performed, the connections discovered are assumed as some kind of brain fingerprint, the so-called default-mode network. Caution must be taken on the confounding effects of the ambient noise, the respiratory and cardiac cycles. One strong reason for resting state fMRI experiments is that they do not impose constraints on the cognitive abilities of the subjects. For instance in pediatric applications, such as the study of brain maturation [14], there is no single cognitive task which is appropriate across the aging population. Several machine learning and data mining approaches have been taken: hierarchical clustering [3], independent component analysis (ICA) [5,16], fractional amplitude of low frequency analysis [23], multivariate pattern analysis (MVPA) [14,15]. Graph analysis has been suggested [17] as a tool to study the connectivity structure of the brain. Resting state fMRI has being found useful for performing studies on brain evolution based on the variations in activity of the default mode network [14], depression (using regional homogeneity measures) [20], Alzheimer's Disease [10], and schizophrenia.

Schizophrenia is a severe psychiatric disease that is characterized by delusions and hallucinations, loss of emotion and disrupted thinking. Functional disconnection between brain regions is suspected to cause these symptoms, because of known aberrant effects on gray and white matter in brain regions that overlap with the default mode network. Resting state fMRI studies [12,21,22] have indicated aberrant default mode functional connectivity in schizophrenic patients. These studies suggest an important role for the default mode network in the pathophysiology of schizophrenia. Functional disconnectivity in schizophrenia could be expressed in altered connectivity of specific functional connections and/or functional networks, but it could also be related to a changed organization of the functional brain network. Resting state studies for schizophrenia patients with auditory hallucinations have also been performed [19] showing reduced connectivity.

3 The Lattice Independent Component Analysis

The linear mixing model can be expressed as follows: $\mathbf{x} = \sum_{i=1}^M a_i \mathbf{e}_i + \mathbf{w} = \mathbf{E}\mathbf{a} + \mathbf{w}$, where \mathbf{x} is the d -dimension pattern vector corresponding to the fMRI voxel time series vector, \mathbf{E} is a $d \times M$ matrix whose columns are the d -dimensional vectors, when these vectors are the vertices of a convex region covering the data they are called endmembers $\mathbf{e}_i, i = 1, \dots, M$, \mathbf{a} is the M -dimension vector of linear mixing coefficients, which correspond to fractional abundances in the convex case, and \mathbf{w} is the d -dimension additive observation noise vector. The linear mixing model is subjected to two constraints on the abundance coefficients when the data points fall into a simplex whose vertices are the endmembers, all abundance coefficients must be non-negative $a_i \geq 0, i = 1, \dots, M$ and normalized to unity summation $\sum_{i=1}^M a_i = 1$. Under this circumstance, we expect that the vectors in \mathbf{E} are affinely independent and that the convex region defined by them includes *all* the data points. Once the endmembers have been determined the unmixing process is the computation of the matrix inversion that gives the coordinates of the point relative to the convex region vertices. The simplest approach is the unconstrained least squared error (LSE) estimation given by: $\hat{\mathbf{a}} = (\mathbf{E}^T \mathbf{E})^{-1} \mathbf{E}^T \mathbf{x}$. Even when the vectors in \mathbf{E} are affinely independent, the coefficients that result from this estimation do not necessarily fulfill the non-negativity and unity normalization. Ensuring both conditions is a complex problem.

The *Lattice Independent Component Analysis* (LICA) is defined by the following steps:

1. Induce from the given data a set of Strongly Lattice Independent vectors. In this paper we apply the Incremental Endmember Induction Algorithm (IEIA) [11,7]. These vectors are taken as a set of affine independent vectors. The advantages of this approach are (1) that we are not imposing statistical assumptions, (2) that the algorithm is one-pass and very fast because it only uses comparisons and addition, (3) that it is unsupervised and incremental, and (4) that it detects naturally the number of endmembers.
2. Apply the unconstrained least squares estimation to obtain the mixing matrix. The detection results are based on the analysis of the coefficients of this matrix. Therefore, the approach is a combination of linear and lattice computing: a linear component analysis where the components have been discovered by non-linear, lattice theory based, algorithms.

4 A Resting State fMRI Case Study

The results shown in this section are explorations over resting state fMRI data obtained from a healthy control subject and an schizophrenia patient with auditory hallucinations selected from an on-going study in the McLean Hospital. Details of image acquisition and demographic information will be given elsewhere. For each subject we have 240 BOLD volumes and one T1-weighted anatomical image. The functional images were coregistered to the T1-weighted anatomical image. The data preprocessing begins with the skull extraction using the BET tool from

FSL (<http://www.fmrib.ox.ac.uk/fsl/>). Further preprocessing, including slice timing, head motion correction (a least squares approach and a 6-parameter spatial transformation), smoothing and spatial normalization to the Montreal Neurological Institute (MNI) template (resampling voxel size = 3.5 mm \times 3.5 mm \times 3.5 mm), were conducted using the Statistical Parametric Mapping (SPM8, <http://www.fil.ion.ucl.ac.uk/spm>) package. Results of LICA and ICA have been computed in Matlab. Visualization of results has been done in FSL. Because both ICA and LICA are unsupervised in the sense that the pattern searched is not predefined, they suffer from the identifiability problem: we do not know beforehand which of the discovered independent sources/endmembers will correspond to a significant brain connection. Therefore, results need a careful assessment by the medical expert. We will not give here any neurological conclusion.

The application of LICA with nominal parameters give 8 endmembers. Accordingly we have computed fastICA setting the number of independent sources to 8. We compute the LICA abundance distributions. For each endmember, we set the 95% percentile of its abundance distribution as the threshold for the detection of the corresponding endmember in the abundance volume. We do the

Table 1. Pearson's Correlation coefficients between ICA and LICA source/endmember detections for the schizophrenia patient

LICA	ICA							
	#1	#2	#3	#4	#5	#6	#7	#8
#1	0.02	0	-0.04	-0.02	0.02	0.03	0.01	0.01
#2	0.03	0.08	-0.1	-0.04	0	0.01	-0.33	0
#3	-0.01	0.36	0.01	-0.07	-0.01	-0.02	0.13	-0.01
#4	0.03	0	-0.03	-0.11	0	-0.01	0	-0.01
#5	-0.03	-0.02	0.16	-0.01	-0.01	-0.11	-0.02	0.46
#6	0.38	-0.03	0.01	-0.13	0.17	0	-0.01	0.01
#7	0	-0.02	0.06	-0.02	-0.01	-0.02	-0.02	-0.01
#8	0.25	0.01	-0.22	0.04	-0.52	0.05	0.02	-0.05

Table 2. Pearson's Correlation coefficients between ICA and LICA source/endmember detections for the healthy control

LICA	ICA							
	#1	#2	#3	#4	#5	#6	#7	#8
#1	0.04	-0.02	-0.04	0.05	-0.06	-0.07	0.03	0.01
#2	-0.02	0.02	0	-0.08	-0.03	-0.03	0.15	-0.01
#3	0.22	-0.05	0.13	0.06	0.01	0.08	-0.03	0.07
#4	0.05	-0.22	0.06	-0.09	0.06	0.08	0.08	-0.03
#5	0.03	0.07	-0.07	0.12	0.14	-0.13	0.04	-0.01
#6	0.04	0	0.05	-0.06	-0.1	0.02	-0.05	-0.03
#7	0.08	0.1	0	0.03	-0.03	-0.02	0.09	0.03
#8	-0.02	-0.04	0.02	0.04	-0.05	-0.07	0.07	0.03

same with the ICA mixture distributions. To explore the agreement between ICA and LICA detections, we have computed the Pearson's correlation between the abundance/mixing volumes of each source/endmember, shown in table 1 for the schizophrenia patient and in table 2 for the control subject. In both cases, agreement between detections of LICA and ICA is low. The best correlation is ICA #8 versus LICA #5 for the schizophrenia patient. For a visual assessment of the agreement between both detection analysis, we show in figure 1 the detections obtained by both algorithms applying the 95% percentile on their respective mixing and abundance coefficients. In this figure, the detection found by LICA is highlighted in blue and the detection found by ICA in red. Overlapping voxels appear in a shade of magenta. It can be appreciated that the LICA detections appear as more compact clusters. Some spurious detections are shown in the surroundings of the brain due to the diffusion produced by the smoothing filter. From these results is clear that we can not use ICA to validate the findings of LICA.

For further comparison, we have computed the correlations intra-algorithm of the patient versus the control data, meaning that we compute the correlations of the abundance/mixing volumes obtained by the LICA/ICA on the patient and the control data. The aim is to get an idea of the ability of each approach to produce discriminant features. If we find negative correlations of high magnitude then we can say that the corresponding approach has a great potential to generate features that discriminate patients from controls. Table 3 shows the correlations between the LICA abundances obtained from the patient and the control subject. Table 4 shows the same information for the mixing coefficients of ICA. In these tables we are interested in finding the most negatively correlated detections, implying complementary detections. We have highlighted in bold the negative correlations below -0.15 . We show in figure 2 the detections with greatest negative correlation between patient and control for both LICA and ICA. In this figure, red corresponds to the patient volume detection, blue corresponds to the control volume detection. Notice again that LICA detections produce more compact clusters. The greatest discrimination is obtained by LICA.

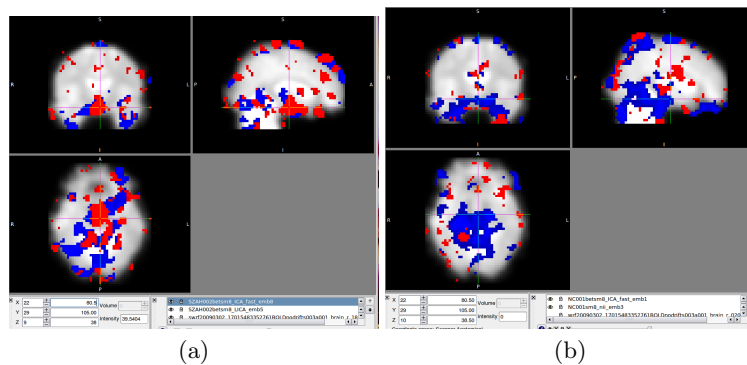


Fig. 1. Simultaneous visualization of the best correlated detection results from LICA and ICA from tables 1 and 2. Red corresponds to ICA detection, Blue to LICA detection. (a) Patient, (b) Control.

Table 3. Correlation between patient and control detections obtained by LICA

control	patient							
	#1	#2	#3	#4	#5	#6	#7	#8
#1	-0.17	-0.04	-0.03	0.24	0.08	0.08	0.09	0.01
#2	0.02	-0.21	0.04	0.1	0.15	0.09	0.02	-0.09
#3	-0.32	0.05	-0.05	0.14	0.24	0.13	0.13	0.15
#4	0.01	0.15	0.08	0.05	-0.03	0.02	0.05	0.17
#5	-0.14	-0.13	-0.18	0.13	0.14	0.11	0.12	-0.04
#6	0.01	-0.06	0.11	0.02	0.02	0.02	-0.02	-0.02
#7	0.06	-0.11	-0.05	-0.15	-0.05	-0.05	-0.12	0.03
#8	-0.32	-0.19	-0.02	0.23	0.22	0.2	0.05	0.02

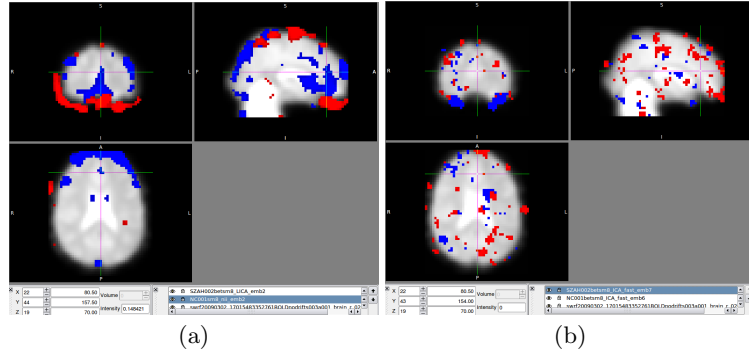


Fig. 2. Findings in the patient versus the control. Greatest negative correlated detections (a) found by LICA, (b) found by ICA.

Table 4. Correlation between patient and control detections obtained by ICA

control	patient							
	#1	#2	#3	#4	#5	#6	#7	#8
#1	0.41	0.01	-0.15	0.01	-0.18	0.02	0.02	-0.04
#2	-0.12	0.02	0.06	-0.04	0.08	-0.01	0.01	0.05
#3	0.02	-0.02	-0.24	-0.02	0.01	0.01	0	0.03
#4	0.03	0	0	0	0.02	0.02	0.02	0
#5	0.04	-0.01	0.06	-0.03	-0.05	-0.01	0.01	0.36
#6	0.04	0.07	-0.05	0.01	0	0	-0.25	0
#7	0.03	0	-0.02	0	-0.01	0.06	0	-0.03
#8	0.02	0.03	-0.01	0	-0.02	0	0.01	0

5 Summary and Conclusions

We are exploring the application of Lattice Independent Component Analysis (LICA) to resting state fMRI. We present results on selected subjects from a study under way in the McLean Hospital. We compare LICA and ICA findings in the form of detections based on the thresholding of the abundance images and mixing matrices. Both LICA and ICA are unsupervised approaches, so they do not force *a priori* assumptions on the localization of the findings, which must be interpreted after the analysis, risking to obtain results not in agreement with the expectations of the analysis. LICA detections are less sparse than those of ICA, but the medical assessment of findings is being carried out actually. The main quantitative conclusion of this study is that there is little agreement between LICA and ICA on this data. Moreover, when we consider the correlation of findings by LICA or ICA on the control versus the schizophrenic patient, we find that the LICA results show greater negative correlation than the results of ICA. We interpret this result as pointing to a greater capability to produce features for discrimination between control and patients based on resting state fMRI data. Anyway, we can not use ICA results as a validation reference, so validation of LICA results must rest on the medical expert assessment of its findings.

References

1. <http://www.cis.hut.fi/projects/ica/fastica/>
2. Chyzyk, D., Termenon, M., Savio, A.: A Comparison of VBM Results by SPM, ICA and LICA. In: Corchado, E., Graña Romay, M., Manhaes Savio, A. (eds.) HAIS 2010. LNCS, vol. 6077, pp. 429–435. Springer, Heidelberg (2010)
3. Cordes, D., Haughton, V., Carew, J.D., Arfanakis, K., Maravilla, K.: Hierarchical clustering to measure connectivity in fmri resting-state data. *Magnetic Resonance Imaging* 20(4), 305–317 (2002)
4. Craddock, R.C., Holtzheimer III, P.E., Hu, X.P., Mayberg, H.S.: Disease state prediction from resting state functional connectivity. *Magnetic Resonance in Medicine* 62, 1619–1628 (2009)
5. Demirci, O., Stevens, M.C., Andreasen, N.C., Michael, A., Liu, J., White, T., Pearlson, G.D., Clark, V.P., Calhoun, V.D.: Investigation of relationships between fMRI brain networks in the spectral domain using ICA and granger causality reveals distinct differences between schizophrenia patients and healthy controls. *NeuroImage* 46(2), 419–431 (2009)
6. Graña, M.: A brief review of lattice computing. In: Proc. WCCI, pp. 1777–1781 (2008)
7. Graña, M., Chyzyk, D., García-Sebastián, M., Hernández, C.: Lattice independent component analysis for functional magnetic resonance imaging. *Information Sciences* (2010) (in press)
8. Graña, M., Savio, A.M., Garcia-Sebastian, M., Fernandez, E.: A lattice computing approach for on-line fmri analysis. *Image and Vision Computing* (2009) (in press)
9. Schmalz, M.S., Ritter, G.X., Urcid, G.: Autonomous single-pass endmember approximation using lattice auto-associative memories. *Neurocomputing* 72(10-12), 2101–2110 (2009)

10. Liu, Y., Wang, K., Yu, C., He, Y., Zhou, Y., Liang, M., Wang, L., Jiang, T.: Regional homogeneity, functional connectivity and imaging markers of alzheimer's disease: A review of resting-state fmri studies. *Neuropsychologia* 46(6), 1648–1656 (2008); *Neuroimaging of Early Alzheimer's Disease*
11. Maldonado, J.O., Hernandez, C., Graña, M., Villaverde, I.: Two lattice computing approaches for the unsupervised segmentation of hyperspectral images. *Neurocomputing* 72(10-12), 2111–2120 (2009)
12. Mingoia, G., Wagner, G., Langbein, K., Scherpiet, S., Schloesser, R., Gaser, C., Sauer, H., Nenadic, I.: Altered default-mode network activity in schizophrenia: A resting state fmri study. *Schizophrenia Research* 117(2-3), 355–356 (2010); 2nd Biennial Schizophrenia International Research Conference
13. Northoff, G., Duncan, N.W., Hayes, D.J.: The brain and its resting state activity—experimental and methodological implications. *Progress in Neurobiology* 92(4), 593–600 (2010)
14. Dosenbach, N.U.F., et al.: Prediction of individual brain maturity using fmri. *Science* 329, 1358–1361 (2010)
15. Pereira, F., Mitchell, T., Botvinick, M.: Machine learning classifiers and fMRI: A tutorial overview. *NeuroImage* 45(supplement 1), S199–S209 (2009); *Mathematics in Brain Imaging*
16. Remes, J.J., Starck, T., Nikkinen, J., Ollila, E., Beckmann, C.F., Tervonen, O., Kiviniemi, V., Silven, O.: Effects of repeatability measures on results of fmri sica: A study on simulated and real resting-state effects. *NeuroImage* (2010) (in Press) Corrected proof
17. van den Heuvel, M.P., Pol, H.E.H.: Exploring the brain network: A review on resting-state fmri functional connectivity. *European Neuropsychopharmacology* 20(8), 519–534 (2010)
18. Calhoun, T.V.D., Adali, T.: Unmixing fmri with independent component analysis. *IEEE Engineering in Medicine and Biology Magazine* 25(2), 79–90 (2006)
19. Vercammen, A., Knegtering, H., den Boer, J.A., Liemburg, E.J., Aleman, A.: Auditory hallucinations in schizophrenia are associated with reduced functional connectivity of the temporo-parietal area. *Biological Psychiatry* 67(10), 912–918 (2010); *Anhedonia in Schizophrenia*
20. Yao, Z., Wang, L., Lu, Q., Liu, H., Teng, G.: Regional homogeneity in depression and its relationship with separate depressive symptom clusters: A resting-state fmri study. *Journal of Affective Disorders* 115(3), 430–438 (2009)
21. Zhou, Y., Liang, M., Jiang, T., Tian, L., Liu, Y., Liu, Z., Liu, H., Kuang, F.: Functional dysconnectivity of the dorsolateral prefrontal cortex in first-episode schizophrenia using resting-state fmri. *Neuroscience Letters* 417(3), 297–302 (2007)
22. Zhou, Y., Shu, N., Liu, Y., Song, M., Hao, Y., Liu, H., Yu, C., Liu, Z., Jiang, T.: Altered resting-state functional connectivity and anatomical connectivity of hippocampus in schizophrenia. *Schizophrenia Research* 100(1-3), 120–132 (2008)
23. Zou, Q.-H., Zhu, C.-Z., Yang, Y., Zuo, X.-N., Long, X.-Y., Cao, Q.-J., Wang, Y.-F., Zang, Y.-F.: An improved approach to detection of amplitude of low-frequency fluctuation (alf) for resting-state fmri: Fractional alf. *Journal of Neuroscience Methods* 172(1), 137–141 (2008)